Switching and measuring a force of 25 femtoNewtons with an optical trap

Alexander Rohrbach

European Molecular Biology Laboratory, Meyerhofstrasse 1, 69117 Heidelberg, Germany
rohrbach@embl.de, rohrbach@imtek.de

http://www.embl.de/~rohrbach

Abstract: An experiment is described, where an ultra-weak force of 25 femtoNewtons (fN = 10^{-15} N) displaces a 0.53µm latex bead captured in a soft optical trap. The displacement is measured by exploiting the phase anomaly of the trapping beam, resulting in a small phase shift of the scattered light. The 25fN force stems from the radiation pressure of a nearly collimated second laser beam, which is switched by an accousto-optical modulator. To the best of my knowledge, this is the smallest switchable force which has ever been directly measured.

OCIS Codes: (140.7010) Trapping; (300.2530) Fluorescence, laser-induced; (290.2200) Extinction; (290.4020) Mie theory; (260.3160) Interference

References

1. A. Ashkin, "Acclearation and trapping of particles by radiation pressure," Phys. Rev. Lett. **24**, 156-159 (1970).
2. H. A. Kramers, "Brownian motion in a field of force and the diffusion model of chemical reactions," Physica **VII**, 284-304 (1940).
3. K. C. Neuman, and S. M. Block, "Optical trapping," Rev. Sci. Instr. **75**, 2787-2809 (2004).
4. R. A. Millikan, "A new modification of the cloud method of. determining the elementary electric charge and the most. probable value of that charge," Philosophical Magazine **19**, 209-228 (1910).
5. D. Rudhardt, C. Bechinger, and P. Leiderer, "Repulsive depletion interactions in colloid–polymer mixtures," J. Phys.: Condens. Matter **11**, 10073–10078 (1999).
6. Y. Matsuo, H. Takasaki, J. Hotta, and K. Sasaki, "Absorption analysis of a single microparticle by optical force measurement," Journal of Applied Physics **89**, 5438-5441 (2001).
7. J. C. Meiners, and S. R. Quake, "Femtonewton force spectroscopy of single extended DNA molecules," Phys. Rev. Lett. **84**, 5014-5017 (2000).
8. G. M. Wang, E. M. Sevick, E. Mittag, D. J. Searles, and D. J. Evans, "Experimental demonstration of violations of the second law of thermodynamics for small systems and short time scales," Phys. Rev. Lett. **89**, -(2002).
9. J. Y. Shao, "Finite element analysis of imposing femtonewton forces with micropipette aspiration," Ann. Biomed. Eng. **30**, 546-554 (2002).
10. A. Rohrbach, "Stiffness of optical traps: Quantitative agreement between experiment and electromagnetic theory," Phys. Rev. Lett. **95**, 168102 (2005).
11. C. Jung, and B. K. Rhee, "Simultaneous determination of thickness and optical constants of polymer thin film by analyzing transmittance," Appl. Opt. **41**, 3861-3865 (2002).
12. A. Rohrbach, C. Tischer, D. Neumayer, E. L. Florin, and E. H. K. Stelzer, "Trapping and tracking a local probe with a Photonic Force Microscope," Rev. Sci. Instrum. **75**, 2197-2210 (2004b).
13. A. Rohrbach, H. Kress, and E. H. K. Stelzer, "Three-dimensional tracking of small spheres in focused laser beams: influence of the detection angular aperture," Opt. Lett. **28**, 411 - 413 (2003).
14. J. K. Dreyer, K. Berg-Sorensen, and L. Oddershede, "Improved axial position detection in optical tweezers measurements," Appl. Opt. **43**, 1991-1995 (2004).
15. A. Pralle, M. Prummer, E.-L. Florin, E. H. K. Stelzer, and J. K. H. Hörber, "Three-dimensional position tracking for optical tweezers by forward scattered light," Microscopy Research and Techniques **44**, 378-386 (1999).
16. A. Rohrbach, and E. H. K. Stelzer, "Three-dimensional position detection of optically trapped dielectric particles," J. Appl. Phys. **91**, 5474-5488 (2002b).
17. C. Bohren, and D. R. Huffman, *Absorption and scattering of light by small particles* (Wiley Science Paperback, New York, 1998).
18. H. C. van de Hulst, *Light Scattering by Small Particles* (Dover Publications, Inc., Leiden, 1957).

#9168 - $15.00 USD Received 18 October 2005; revised 10 November 2005; accepted 10 November 2005

1. Introduction

Although photons are massless, they can exert a pressure on matter, by transferring their momentum h/λ, which is the inverse incident wavelength quantized by Planck's constant. Although one photon carries a tiny momentum of 6.626×10^{-28} Ns at a wavelength of $\lambda = 1$ µm, this momentum sums up to a gigantic radiation pressure in the center of hot stars. This pressure works against the gravitational forces, which would induce a collapse of the star. In principle the photon momentum can be exploited for an interplanetary transport of space-ships with solar sails. Large, photon reflecting surfaces (sails) with low mass, are slowly, but almost frictionless accelerated by the photon flux emitted by the sun. This situation changes completely in the earth's atmosphere, where collisions with air molecules dissipate the kinetic energy of the objects accelerated by radiation pressure. The question arises by how far these forces can be scaled down to laboratory situations.

Already 1970 Ashkin [1] dragged micron-sized latex spheres with an Argon laser and measured radiation forces in the picoNewton (pN) range by finding the equilibrium of optical and friction forces. However, the smaller and lighter the optically accelerated particles, the more pronounced becomes the viscous drag force $\gamma \cdot v$ and thermal random forces F_{th} (leading to Brownian motion). For example, a 1µm latex bead can take up a kinetic or thermal energy of 8 k_BT ($k_BT \approx 4 \cdot 10^{-21}$Nm at T = 300 K, k_B = Boltzmann constant) after a few seconds [2]. By moving over a distance of e.g. $\Delta x = 30$nm against an external potential W(x), the effective thermal force can easily become $F_{th} = \partial_x^2 W(x) \cdot \Delta x = 1$ pN. The gravity $G = m \cdot g$ of this bead is only 10 fN. A molecular motor transporting this 1µm bead along fibers in a living cell exerts forces of 3-5 pN in this Brownian storm of thermal forces. Forces in the pN regime have been successfully measured with optical tweezers (see review of Neuman and Block [3]), whereas direct force measurements in the low fN regime are very difficult to perform. With a direct measurement of a force F_{mes} I refer to the equilibration with a single calibrated force $F_{cal} = F_{mes}$.

Where do we find fN forces? For instance, the entropic force that arises when the entropy is reduced by stretching e.g. a DNA polymer with a persistence length of $L_p = 50$ nm is $F_{ent} = k_BT/L_p = 80$ fN. A 1µm small bacterium has to overcome a friction force of $F_{fr} = \gamma \cdot v = 95$ fN at a propagation speed of v = 10 µm/s in water. The gravitational attraction between two 3 mm glass spheres close to each other is about 10 fN. The repulsive electrostatic force of a 0.5 µm latex sphere in de-ionized water is about 20 fN in a distance of 1.5 µm to the surface due to the auto-dissociation of water. In his famous experiments to prove the quantization of electric charge [4], Millikan switched a 100-200 fN small electric force $F_E = E \cdot n \cdot q$ to counterbalance the gravitational force $m \cdot g$ on 3-4 µm sized oil drops, loaded with n elementary charges q. And coming back to the radiation pressure, the daily sun light, defined by the solar intensity $I_{sol} = 1370$ W/m^2 exerts a force

$$F_{rad} = I_0 \cdot n/c \cdot Q_{pr} \cdot (a^2\pi) \qquad (1)$$

of only 20 fN on a small absorbing dust particle of $2a = 75$µm in diameter in the atmosphere. $I_0 = I_{sol}$ is the intensity incident on the particle's cross-section ($a^2\pi$), c/n is the speed of light in a medium with refractive index n and Q_{pr} is the pressure efficiency, which is 1 for an absorbing particle. I have setup an arbitrary collection of ultra-small forces to give the reader a feeling for magnitudes in the low femtoNewton range.

#9168 - $15.00 USD Received 18 October 2005; revised 10 November 2005; accepted 10 November 2005

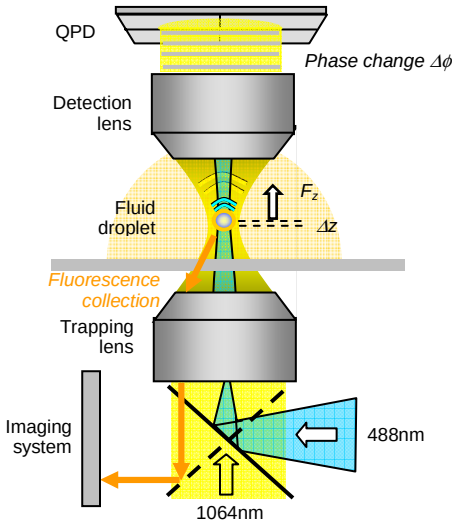

Fig. 1. Experimental setup. A collimated IR beam (1064nm) is focused by NA = 1.2 water immersion lens. A 535nm latex sphere is trapped weakly and scatters the incident IR light coherently. The detection lens dipping into the fluid droplet collects both the scattered and unscattered light, which have a phase difference of $\Delta\phi$ to each other. A quadrant photo diode (QPD) records the interference pattern, which changes with $\Delta\phi$. The fluid droplet consists of a fluorescein solution. A 488nm laser is switched on, resulting in an axial displacement of the trapped bead by Δz and an phase shift $\Delta\phi(\Delta z)$ of the IR light due to radiation pressure. The fluorescence light emitted along the 488nm beam profile is recorded by the imaging system.

Force measurements in the low femtoNewton range are mentioned regularly in the literature [5-9], but attention has to be paid, whether these studies present a direct measurement or an estimation of the apparatus' resolution for force measurements.

So far no report has been found in the literature where such small forces could be controlled and measured directly. In this paper I demonstrate how a force of 25 fN on a small probe is switched and measured directly with help of an ultra-weak optical trap and an interferometric position detection system. The force can be switched on and off, such that no extrapolation of a system inherent force distribution is necessary. Only two parameters need to be determined for the measurement: the stiffness κ_z of the optical trap [10], which is obtained by signal autocorrelations $\langle S_z(t)\cdot S_z(t+\tau)\rangle$ of the probe's position z(t), and secondly, the shift Δz of the probe's mean position, measured before and after the femtoNewton force was switched on. The measured force is then $F_z = \kappa_z\cdot\Delta z$. The displacement Δz is obtained via the tiny phase change of the trapping beam scattered at the probe.

2. Instrumentation and experiment

Which femtoNewton force can be quickly switched on and off and leaves the system in thermal equilibrium in both the on- and off-state? A conservative force, which can be easily controlled, results from the radiation pressure of a collimated laser beam on a non-absorbing sphere. A 488nm Argon laser beam was switched with a accousto-optical modulator (AOM) leading to an optical power of P = 11 mW at the dielectric probe, which was a 0.535 µm latex bead with refractive index $n_s = 1.591+0.0003i$ [11].

The ultra-low force measurement was performed with a photonic force microscope (PFM), which is an optical tweezers related system with a 3D interferometric probe tracking system. Technical details of the PFM are described elsewhere [12]. The experimental setup is illustrated by Fig. 1. An unexpanded 488nm laser beam is weakly focused into the back focal plane (BFP) of the trapping lens. This results in a nearly collimated beam with waist s in the focal plane of the trapping lens. A trapped latex bead with radius a = 268 nm (Bangs Labs

#9168 - $15.00 USD Received 18 October 2005; revised 10 November 2005; accepted 10 November 2005

Inc.) is moved in axial direction by the radiation pressure of the 488nm laser beam, until the radiation force of the 488nm beam equilibrates with the trapping force of the 1064nm beam.

The trapping force F_{trap} is obtained by calibrating both the optical trap and the detection system. The axial force $F_{trap} = \kappa_z \cdot \Delta z$ is calibrated by the axial stiffness $\kappa_z = \gamma/\tau_z$ and the detection system is calibrated by the axial signal sensitivity $g_z = \sigma_{sz} / \sigma_z = \sigma_{sz} \cdot (\kappa_z/k_BT)^{1/2}$ of the particle's position signal $S_z(z) = g_z \cdot z$, which is linear to the position z over a reasonable distance [12]. The mean square displacement of the trapped particle $\sigma_z^2 := \langle \sigma_z(t)^2 \rangle$ follows the equipartition theorem $\kappa_z \cdot \sigma_z^2 = k_BT$. The resulting half width σ_{sz} of the signal histogram (Fig. 2(b)) is obtained by a Gaussian fit $\exp[-(S_z/\sigma_{sz})^2]$. The autocorrelation time τ_z is the time the particle needs to relax inside the optical trap in axial direction and is provided by the signal autocorrelations $\langle S_z(t) \cdot S_z(t+\tau) \rangle = \langle |S_z(0)|^2 \rangle \exp(-\tau/\tau_z)$. $\gamma = 6\pi a\eta$ is the viscous drag far from an interface (η viscosity of water). Therefore the relation between the particle's position z(t) and it's position signal $S_z(z(t))$ is

$$S_z(z) \approx g_z \cdot z = \sigma_{sz} \cdot [\gamma/(\tau_z \cdot k_BT)]^{1/2} \cdot z. \tag{2}$$

Therefore the radiation force from the 488nm laser is provided by the force equilibrium

$$F_{rad} = F_{trap}(\Delta z) = \kappa_z \cdot \Delta z = \kappa_z \cdot \Delta S_z / g_z = \Delta S_z / \sigma_{sz} \cdot (\kappa_z \cdot k_BT)^{1/2} \tag{3}$$

The axial displacement of the particle Δz is proportional to the difference ΔS_z in the mean position signals

$$\Delta S_z = \langle S_{on} \rangle - \langle S_{off} \rangle = \tfrac{1}{\Delta T_{on}} \int_{\Delta T_{on}} S_{z,on}(t)\, dt - \tfrac{1}{\Delta T_{off}} \int_{\Delta T_{off}} S_{z,off}(t)\, dt \tag{4}$$

The position signal $S_z(t) = \langle S \rangle \pm \sigma_{sz}(t)$ fluctuates by $\sigma_{sz}(t) = g_z \cdot \sigma_z(t)$ around the mean value $\langle S \rangle$ due to thermal motion (see Fig. 2(a)). The integration times were $\Delta T_{on} \approx \Delta T_{off} \approx 4$s at a sampling rate of 50 kHz. The temperature was T = 21°C.

The signals S_z are acquired by integrating the interference intensity over the full area of the QPD [12], the signal sensitivity $g_z(NA_{det})$ can be increased by decreasing the numerical aperture of the detection lens NA_{det} [13, 14], which we reduced to $NA_{det} = 0.3$. S_z is the integrated interference intensity between the incident field $\mathbf{E}_i$ and the scattered field $\mathbf{E}_s(z)$ which varies with the position of the probe z.

$$S_z(z) = \int \left| E_i + E_s(z) \right|^2 dA = \int \left(|E_i|^2 + |E_s(z)|^2 + |E_i|\,|E_s(z)| \cos(\phi_i - \phi_s(z)) \right) dA \tag{5}$$

Close to the focus, the phase difference $\Delta\phi(\Delta z) = \phi_i - \phi_s(\Delta z) \sim \Delta z$ is proportional to the particle's displacement Δz due to the Gouy phase shift [15, 16]. The Gouy phase shift leads to the reduced momentum carried by a focused beam in axial direction. Via a phase shift of π it leads to a stretching of the mean wavelength in the focal area.

Once the detection system is calibrated, i.e. $g_z = \Delta S_z / \Delta z$ has been determined, an alternative way to gain the radiation force is to subtract the off-state potential $V_{off}(z)$ from the on-state potential $V_{on}(z) = V_{off}(z) + V_{rad}(z)$. The potentials V(z) are related to the probability density p(z) of the histograms via Boltzmann statistics $p(z) \sim \exp[-V(z)/k_BT]$. The radiation force then is the derivative of the radiation potential, i.e. $F_{rad} = \partial/\partial z\, V_{rad}(z)$. This method is illustrated in Fig. 2(c).

#9168 - $15.00 USD Received 18 October 2005; revised 10 November 2005; accepted 10 November 2005

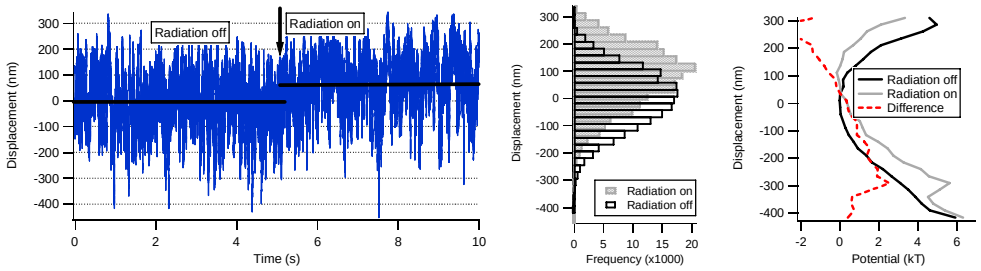

(a) (b) (c)

Fig. 2. Axial bead displacements and histograms. (a) The 535nm latex bead fluctuates inside the weak optical trap. By switching on an additional radiation pressure after about 5 sec, the mean position of the bead changes by 70nm. (b) The histograms illustrate the ratio between the mean displacements due to thermal noise and due to the ultra-weak external force. The widths of the histograms σ_{sz} are nearly the same in both cases. (c) The radiation force can also be obtained from the difference in the corresponding potentials.

To estimate the number of photons transferring their momentum on to the probe, the intensity I_0 of the 488nm laser beam at the probe was determined. As illustrated in Fig. 1, a diluted fluorescein solution (mass ratio $2 \cdot 10^{-5}$) was used to measure the beam waist s of the beam. After fluorescence excitation, the beam profile was imaged onto a CCD camera (see Fig. 3). The axial extent of the focus, i.e. the extent of the detection plane (focal plane) is about 1µm, whereas the Rayleigh length of the beam is much longer, ensuring that no artifact is introduced by the integration of the detection lens. By fitting a Gaussian beam profile to the fluorescence intensity $I(r) = I_0 \cdot \exp(-r^2/s^2)$, a half width of s = 7µm at I_0/e was obtained (Fig. 3 left). The trapped probe was well centered relative to the 488nm beam, as indicated in Fig. 3 right. Here the fluorescence increase due to coherent scattering behind the sphere is 70%, integrated over the depth of field of the trapping lens.

3. Results and discussion

The total power P_{488} = 11 mW in the focal plane is 62% of the power measured behind the coverslip without the trapping lens. P is distributed over the whole focal plane according to

$$P_{488} = \int_0^\infty I(r) \cdot 2\pi r \, dr = I_0 2\pi \int_0^\infty \exp(-r^2/s^2) \cdot r \, dr = I_0 \cdot s^2 \cdot \pi \qquad (6)$$

From Eq. (6) we find $I_0 = P_{488} / (\pi s^2) = 71.5$ MW/m^2, which corresponds to a power of $P_{geo} = I_0 \cdot a^2\pi$ = 16.1 µW distributed over the cross section of the sphere, which is $C_{geo} = a^2\pi$ = 0.226 µm^2. In other words $P_{geo}/(h\nu) \approx 5.3 \cdot 10^{13}$ photons per second hit the sphere's cross section.

The resulting radiation force can be measured by using eq.(3). Totally 11 measurements were performed at two strengths of the optical trap (λ_{trap} = 1064nm). At a very low trapping laser power P_{trap} = 1.5mW in the focal plane, a radiation force of F_{rad} = 25.6 ± 2.2 fN was obtained (N=5 measurements). This force is the product of a mean trap stiffness of κ_z = 0.37 pN/µm and a mean displacement Δz = 69nm. At a second, still low laser power P_{trap} = 4.4mW nearly the same radiation force of F_{rad} = 22.3 ± 5.7 fN was measured (N=6), which is the product of a mean trap stiffness of κ_z = 1.12 pN/µm and a mean displacement Δz = 20nm. The consistency and the relative small errors underline the reliability of the measurements. The uncertainty in the force measurement due to thermal fluctuations is $F \pm \Delta F = \kappa_z \cdot (\Delta z \pm \sigma_z)$ with

#9168 - $15.00 USD Received 18 October 2005; revised 10 November 2005; accepted 10 November 2005

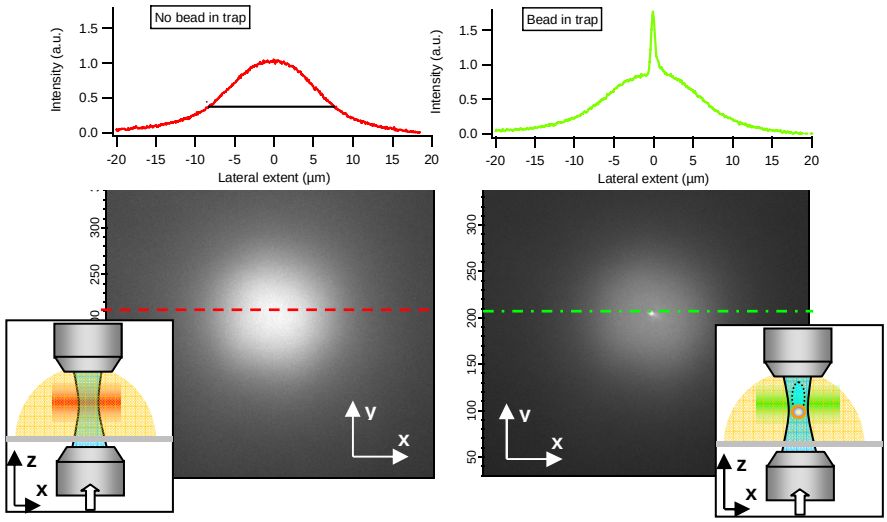

Fig. 3. The Gaussian profile of the weakly focused laser beam is visible due to fluorescence emission in the fluorescein solution (left image). The intensity profile reveals a beam waist of 2s = 14µm at a 1/e decay. Right: A bead trapped in the center of visible laser beam produces an increase in electric field density behind the bead due to scattering. In this region the fluorescence intensity is increased by 70% as indicated by the profile and the photo. Integration time was 20ms.

$\sigma_z^2 = k_B T/\kappa_z$). The uncertainty ΔF increases with $(k_B T\ \kappa_z)^{1/2}$ at a constant external force F_{rad} and can be reduced by using a weak optical trap, i.e. a small trapping stiffness κ_z, and, of course, by a low temperature T. Since resolution is a question of definition, I chose that $\Delta F \leq F$ or $\sigma_z \leq \Delta z$, which was approximately fulfilled in this experiment ($\Delta z \approx \sigma_z \approx 70$nm). By defining a different resolution limit or by achieving an even smaller trap stiffness, forces smaller than 25fN can be measured.

As a further verification, a similar radiation force F_{rad} (< 15% deviation) was determined by the gradient of the potential difference as illustrated in Fig. 2 right. Furthermore, the correctness of the detector calibration g_z via the relaxation time τ_z (eq.(2)) was tested by moving a fixed bead over a distance Δz through the focus by a piezo-stage. The ratio $g_z = \Delta S_z / \Delta z$ provided nearly the same value.

According to Mie-theory, a sphere with index $n_s = n_R + i \cdot n_I = 1.591 + 0.0003i$ and radius a = 268nm has the scattering function $S(\theta=0) = 7.715 - 10.548i$ leading to a scattering efficiency $Q_{sca} = 4/(k \cdot a)^2 \cdot \mathrm{Re}\{S(0)\} = 1.4653$, $k = 2\pi\, n/\lambda$, $\lambda = 488$nm. This would mean that 147% of the incident photons are scattered at the sphere (extinction paradox) [17]. However, due to diffraction, i.e. the redistribution of optical energy and momentum, more photons are scattered in forward direction ($\theta=0$) due to interference with the unscattered field. The resulting pressure efficiency without absorption is $Q_{pr} - Q_{abs} = 0.180$, where

$$Q_{pr} = Q_{abs} + Q_{sca} - \frac{Q_{sca}}{n^2 k_0^2 a^2} \int_0^{\pi} \tfrac{1}{2} \left(|T_1(\theta)|^2 + |T_2(\theta)|^2 \right) \cos\theta \sin\theta \, d\theta \qquad (7)$$

Here n is the refractive index of the medium (water) and Q_{abs} is the absorption efficiency. $T_1(\theta)$ and $T_2(\theta)$ are the angle-dependent Mie-scattering functions parallel and perpendicular to the plane of incidence[18]. Using Eq. (1), we obtain a theoretical radiation pressure of F_{rad} = 12.8fN, if $Q_{abs} = 0$. This theoretical value is only half as large as the measured value for the radiation force. It is therefore likely that absorption takes place at the sphere. The momentum uptake ~ Q_{abs} due to absorption and incoherent scattering must be about the same as due to coherent scattering ~$(Q_{pr} - Q_{abs})$.

#9168 - $15.00 USD Received 18 October 2005; revised 10 November 2005; accepted 10 November 2005

Therefore my colleague Holger Kress (EMBL Heidelberg) proposed and proved the spontaneous adhesion of fluorescein fluorophores at the surface of the bead (Bangs Lab Inc.). Assuming in the simplest case a dense monolayer of fluorophores, we expect a number N of absorbing fluorophores on the front and back side of the bead with geometrical cross-section $C_{geo} = a^2\pi$. With a geometrical cross-section $r^2\pi$ of the fluorophores, the number of molecules is $N = 2a^2\pi / r^2\pi = 2.26 \cdot 10^6$. The diameter of a fluorescein fluorophore is about 2r = 0.5nm and the molar extinction coefficient of fluorescein is about $C_{ext,fl} = 72000\ (mol/l)^{-1}cm^{-1}$ (see Sigma-Genosys, www.fisheroligos.com/tec_flc.htm), which is $C_{ext,fl} = 72000\ m^2/N_A = 0.012\ (nm)^2$ (N_A = Lohschmidt number, $C_{sca,fl} = 0$ due to incoherent, isotropic scattering). This results in a total absorption cross-section of $C_{abs} = N \cdot C_{ext,fl} = 0.034\ \mu m^2$ or an absorption efficiency $Q_{abs} = C_{abs} / C_{geo} = 0.15$, which is about the same as $Q_{pr} - Q_{abs} = 0.18$ due to coherent scattering at the sphere. Again, according to this estimation, a latex sphere with diameter 535nm takes up the same amount of light momentum as a 0.5nm thin monolayer of fluorescein molecules around the sphere. The emitted fluorescence of the dye monolayer is small in comparison to the increased excitation and fluorescence behind the sphere due to coherent scattering of the excitation light.

Some years ago Matsuo et al. [6] tried to exploit the difference between the measured radiation pressure efficiency on a particle and the computed scattering efficiency to estimate the absorption of the particle. However, in this study unique measurements were complicated due to a more complex scattering at the 10-fold larger spheres and the close proximity of two interfaces.

Finally I want to remark that also the absorbance of the 488nm light by fluorophores inside the fluorescein droplet should have an effect on the final momentum transfer, because it mainly reduces I_0 at the sphere. An estimate of this reduction is complicated due to the diffusion of fluorophores through the beam.

Although different ratios of momentum uptake due to resonant and non-resonant scattering at the (coated) sphere may result in a radiation force of 25fN, the force switching and measurement remains unaffected by this ratio.

4. Conclusions

The smallest switchable force ever was measured by using an ultra-weak optical trap. Different measurements manifest a force of about 25 fN resulting from the radiation pressure of a 11mW laser beam (λ = 488nm) on a 0.53µm latex sphere. About half of this force results from momentum transfer due to coherent scattering, the other half is likely due to absorption of a dense monolayer of fluorescein molecules around the sphere. With this study I try to set a new milestone concerning force measurements in the sub-picoNewton regime and I encourage other researchers to underbid this value with careful measurements.

Acknowledgments

I thank Holger Kress for helpful comments, especially for providing the concept of the absorbing monolayer around the sphere and I thank Dr. Ernst H.K. Stelzer for general support.

#9168 - $15.00 USD Received 18 October 2005; revised 10 November 2005; accepted 10 November 2005